

1 **“Snail factors in testicular germ cell tumours and their regulation by the BMP4**
2 **signalling pathway”**

3 Diana J. Micati ^{1,2}, Karthika Radhakrishnan ^{1,2}, Julia C. Young ^{1,2,6}, Ewa Rajpert-De Meyts ³,
4 Gary R. Hime ⁴, *Helen E. Abud ^{5,6}, and *Kate L. Loveland ^{1,2,6}

5 *Helen E Abud and Kate L Loveland are equal senior co-authors

- 6 1. Centre for Reproductive Health, Hudson Institute of Medical Research, Clayton, Victoria, Australia
- 7 2. Department of Molecular and Translational Sciences, Monash University, Clayton, Victoria, Australia
- 8 3. Department of Growth and Reproduction, Rigshospitalet, University of Copenhagen, Denmark
- 9 4. Department of Anatomy and Neuroscience, University of Melbourne, Melbourne, Australia
- 10 5. Stem cells and Development Program, Monash Biomedicine Discovery Institute, Monash University,
- 11 Clayton, Victoria, Australia
- 12 6. Department of Anatomy and Developmental Biology, Monash Biomedicine Discovery Institute, Monash
- 13 University, Clayton, Victoria, Australia

14
15 Correspondence should be addressed to K.L.

16 Phone +61 3 8572-2904

17 Address: Level 4 MHRP, 27-31 Wright Street, Hudson Institute of Medical Research,
18 Clayton, 3168 Australia

19 Email: kate.loveland@monash.edu

20 Running title: Snail transcription factors in human germ cells

21 Funding information: This work was supported by grants from the National Health and
22 Medical Research Council of Australia (Project grant ID1048110 to GH, HA, KL and
23 Fellowship ID1079646 to KL)

24 Keywords: Snail transcription factors, human spermatogenesis, testicular germ cell
25 tumours, TGF- β superfamily, importin 5

26
27 **Abstract**

This is the author manuscript accepted for publication and has undergone full peer review but has not been through the copyediting, typesetting, pagination and proofreading process, which may lead to differences between this version and the [Version of Record](#). Please cite this article as [doi: 10.1111/andr.12823](https://doi.org/10.1111/andr.12823)

This article is protected by copyright. All rights reserved

28 **Background:** Snail transcription factors mediate key cellular transitions in many
29 developmental processes, including spermatogenesis, and their production can be regulated by
30 TGF- β superfamily signalling. SNAI1 and SNAI2 support many cancers of epithelial origin.
31 Their functional relevance and potential regulation by TGF- β superfamily ligands in germ cell
32 neoplasia are unknown.

33 **Methods:** SNAI1, SNAI2 and importin 5 (IPO5; nuclear transporter that selectively mediates
34 BMP signalling) cellular localisation was examined in fixed normal adult human and/or
35 neoplastic testes using *in situ* hybridisation and/or immunohistochemistry. SNAI1 and SNAI2
36 functions were assessed using the well characterised human seminoma cell line, TCam-2. Cell
37 migration, adhesion/proliferation, and survival were measured by scratch assay, xCELLigence
38 and flow cytometry following siRNA-induced reduction of *SNAI1* and *SNAI2* in TCam-2 cells.
39 The potential regulation of *SNAI1* and *SNAI2* in TCam-2 cells by TGF- β signalling ligands,
40 activin A and BMP4, was evaluated following 48 hours culture, including with siRNA
41 regulation of IPO5 to selectively restrict BMP4 signalling.

42 **Results:** In normal testes, *SNAI1* transcript was identified in some spermatogonia and in
43 spermatocytes, and SNAI2 protein localised to nuclei of spermatogonia, spermatocytes and
44 round spermatids. In neoplastic testes, both *SNAI1* and SNAI2 were detected in GCNIS and in
45 seminoma cells. SNAI1 and SNAI2 reduction in TCam-2 cells by siRNAs significantly
46 inhibited migration and survival, respectively. Exposure to BMP4, but not activin A,
47 significantly increased *SNAI2* (~18-fold). *IPO5* inhibition by siRNAs decreased BMP4-
48 induced *SNAI2* upregulation (~5-fold). Additionally, *SNAI2* reduction using siRNAs inhibited
49 BMP4-induced TCam-2 cell survival.

50 **Conclusions:** This is the first evidence that SNAI1 and SNAI2 are involved in human
51 spermatogenesis, with independent functions. These outcomes demonstrate that SNAI1 and
52 SNAI2 inhibition leads to loss of migratory and viability capacities in seminoma cells. These
53 findings show the potential for therapeutic treatments targeting SNAI1 or BMP4 signalling for
54 patients with metastatic testicular germ cell tumours.

55

56

57

58 **Introduction**

59 Snail proteins belong to a family of zinc-finger transcription factors that play crucial roles in
60 cell migration, chromatin remodelling and cell signalling to impact on many biological
61 processes in normal embryonic development and tumorigenesis (1, 2). The three Snail factors
62 exert their functions through tight transcriptional regulation. Their highly conserved C-terminal
63 region contains 4 to 6 zinc fingers in a DNA-binding domain which interacts directly with
64 target genes. Once bound, Snail proteins recruit several co-factors through their N-terminal
65 SNAG domain; these are mainly chromatin remodelling enzymes that directly repress or
66 activate gene activity depending on cell-context (1, 3, 4).

67 There is limited information from studies of the adult mouse testis to suggest Snail factors
68 mediate key cellular transitions by controlling changes in gene expression. In adult mice,
69 aberrant *Snail* or *Snai2* synthesis disrupted spermatogenesis. Specifically, analysis of ubiquitin
70 ligase β -*Trcp* knockout mice provided indirect evidence that elevated SNAI1 in spermatogonia
71 can cause germ cell loss (5). A testicular phenotype was reported in mice lacking *Snai2* at six
72 weeks of age, with testicular atrophy resulting from an apparent reduction in germ cell number
73 (6). However, no further characterisation of these testes is available. We previously identified
74 the precise cellular sites of Snail transcription factor activity in the postnatal mouse testis,
75 revealing distinct and dynamic profiles for each. SNAI1 and SNAI2, not SNAI3, were detected
76 in the nucleus of germ cells at different stages of maturation. They co-localised with chromatin
77 remodelling enzymes, such as LSD1 and PRC2 components (7), and thus mediate
78 transcriptome reprogramming during spermatogenesis (8, 9).

79 Snail functions are well defined in epithelial cells. By regulating epithelial cell gene expression,
80 Snail factors can induce an epithelial to mesenchymal transition (EMT) (10) in which an
81 epithelial cell acquires the migratory and invasive capacities of a mesenchymal cell (11). EMT
82 is required for normal embryonic development, but in adults, Snail-induced reduction of
83 epithelial markers, such as *CDHI*, is a hallmark of tumour initiation, providing cancer cells
84 with the ability to migrate from the primary tumour and metastasise to distant sites (12).

85 Snail activities also contribute to normal tissue homeostasis and cancer progression, as elevated
86 Snail levels drive cells to acquire stem cell properties. In mouse small intestinal epithelium,
87 Snail expression is localised to the stem cell population where it is required for their
88 maintenance (13, 14). Increased Snail levels promote a stem cell-like phenotype in various
89 cancers including those of the breast epithelium (15) and human pancreas (16); this allows
90 cancer cells to adopt self-renewing capacities, become chemotherapy resistant and metastatic

91 and cause relapse (17). Snail overexpression can also increase proliferation of human
92 glioblastoma cells (18) and support survival of two gastrointestinal stromal tumour cell lines
93 by regulating pro-apoptotic and anti-apoptotic gene activity (19). As Snail proteins function
94 beyond EMT, it is evident that they promote cancers of non-epithelial origins, such as testicular
95 germ cell tumours (TGCTs).

96 TGCTs arise from a common precursor cell known as germ cell neoplasia *in situ* (GCNIS),
97 first described as an atypical spermatogonia in testicular biopsies of patients who subsequently
98 developed testicular cancer (20). Similarities in morphology and gene expression profiles
99 between GCNIS and human foetal germ cells indicates that GCNIS originates from an early
100 gonocyte that has failed to differentiate, but persists in adulthood (21, 22). Unknown events
101 that occur at puberty drive GCNIS cells to proliferate and progress into one of the two
102 malignant TGCTs (23): either seminoma or non-seminomas, the latter characterised by loss of
103 germ cell phenotype and activation of somatic differentiation. Among men with TGCTs,
104 approximately 50% are diagnosed with seminomas (24, 25) which histologically appear as
105 undifferentiated cells that resemble GCNIS with characteristic lymphocytic infiltration in the
106 supporting stroma.

107 The Transforming Growth Factor (TGF- β) signalling pathway is central to testis development
108 and reproductive health (26), in addition to embryogenesis and tumorigenesis (27, 28). Briefly,
109 activin A binding to serine/threonine kinase receptor subunits induces phosphorylation of
110 SMADs 2 and/or 3. In contrast, BMP4 binding to cognate receptors, including those shared
111 with activin, leads to phosphorylation of SMAD 1/5/9 (29). Once phosphorylated, SMADs
112 bind to SMAD4 forming a trimeric complex which is transported into the nucleus to activate
113 target gene transcription in concert with specific co-factors (30, 31). Protein transport from the
114 cytoplasm into the nucleus is mediated by importins (32). IPO5 is one of the several importin
115 molecules readily detected in the embryonic and postnatal mouse testis (33, 34), and in the
116 normal adult human testis (35). Its dynamic and cell-specific expression profile suggests that
117 IPO5 plays a role during major developmental switches, potentially influencing testis
118 development and sperm production. Recent studies identified IPO5 as an intracellular mediator
119 of the BMP4 signalling pathway translocates SMADs 1/5/9, but not SMADs 2/3, from
120 cytoplasm to nucleus initiating transcription of BMP4 target genes (36). Thus, the selective
121 transport of SMADs 1/5/9 by IPO5 indicates its expression and function is particularly
122 important as a BMP4 signalling mediator; its presence and role in TGCTs is yet to be
123 elucidated.

124 Several lines of evidence link aberrant TGF- β signalling with TGCT progression. Elevation of
125 the activin A type II receptor in the adult testis is observed only within seminoma cells (37),
126 and upregulation of activin inhibitors, betaglycan and inhibin (38), is also detected in some
127 seminoma samples. This highlights the potential involvement of disrupted activin signalling in
128 TGCT. Altered BMP signalling in TGCT is indicated by BMPR expression in paediatric
129 seminomas/germinomas (39) and mutation in activin receptor-like kinase (*alk6b*), a BMP
130 receptor, in zebrafish germ cell tumours (40). An important model of human seminoma with
131 early gonocyte features, the TCam-2 human seminoma cell line, responds differentially to
132 activin A and BMP4 (41). It features hallmarks of early foetal germ cells and primary
133 seminoma tumours including PRDM1 (BLIMP1), KIT, OCT3/4, SOX17, AP2 γ , and NANOG
134 (42). Activin A treatment of TCam-2 cells significantly increases *KIT* transcript level, while
135 exposure to BMP4 increases survival (41), indicating the TGF- β superfamily pathway regulates
136 transcription of factors associated with germ cell development. Snail transcription factor levels
137 are regulated by the TGF- β superfamily (11) in the uterus to allow extravillous cytotrophoblasts
138 invasion of the endometrium to support placental development (43). In the oesophagus, BMP4-
139 induction of *SNAI2* expression mediate the transformation of premalignant squamous epithelial
140 cells into oesophageal adenocarcinoma (44). However, Snail regulation mediated by activin A
141 or BMP4 in seminomas has not been studied.

142 The present study was performed to investigate how Snail transcription factors may influence
143 TGCT initiation and progression. For the first time, we provide evidence that SNAI1 and
144 SNAI2 are present in germ cells of the normal adult human testis, supporting the hypothesis
145 that Snail transcription factors might regulate gene expression changes at key spermatogenic
146 stages, as previously documented in mice. Identification of SNAI1 and SNAI2 in GCNIS and
147 seminomas suggests that Snail factors contribute to TGCT initiation and progression. To
148 address their functions in cell migration, proliferation, adhesion and survival, TCam-2 cells
149 were used and treatment of TCam-2 cells with activin A and BMP4 identified a potential
150 mechanism for Snail regulation.

151

152 **Materials and Methods**

153 **Histological analysis of normal and neoplastic human testis samples**

154 Snail transcript and protein expression patterns were analysed using 4 μ m thick, Bouin's or
155 PFA fixed, paraffin-embedded sections of normal adult human testis, GCNIS with or without

156 areas of normal spermatogenesis, and seminomas. GCNIS and seminoma tissue samples
157 employed in this study were derived from adult male patients, ranging between 27 and 55 years
158 old. All procedures involving normal adult human testis and TGCT samples were approved by
159 the Monash University Human Research Ethics Committee and the Regional Committee for
160 Medical Research Ethics (Copenhagen), respectively.

161 **DIG-labelled RNA probes and *in situ* hybridisation**

162 DIG-labelled RNA probes for *in situ* hybridisation were originally generated from RT-PCR
163 products (primer sequences in Table 1) cloned into the pGEM-T-Easy vector (Promega,
164 Madison, WI, USA) and validated by sequencing (Gandel Genomics Centre, Monash Health
165 Translation Precinct). These plasmids were amplified by RT-PCR using pBS forward and
166 reverse primers to create templates for *in vitro* transcription to generate sense and antisense
167 cRNA probes.

168 *In situ* hybridisation was used to detect *SNAIL1* and *SNAI2* in Bouin's fixed section of human
169 testis samples used standard procedures (7). In brief, hybridisation was performed with 3 µg/ml
170 probe diluted in *in situ* hybridisation buffer at 55°C overnight. Bound-cRNA probe was
171 detected using an alkaline phosphatase-labelled-anti-DIG antibody (1:1000 in 10 X DIG
172 blocking buffer, Roche) and visualised using a substrate for alkaline phosphatase (BCIP/NBT,
173 Thermo Fisher Scientific). Sections were counterstained with Harris haematoxylin (Sigma-
174 Aldrich) and mounted with GVA aqueous mounting solution (Genemed, San Francisco, CA,
175 USA). *In situ* hybridisation was performed using the *SNAIL1* cRNA probes on 2 and 3 normal
176 adult and neoplastic human samples, respectively. The *SNAI2* antisense cRNA probe was used
177 to detect *SNAI2* transcript in normal adult human testes only. *SNAI2* expression pattern in
178 normal and neoplastic adult human samples was further delineated by immunohistochemistry
179 using an anti-SNAI2 antibody as described below.

180 **Immunohistochemistry**

181 Immunostaining was performed to localise SNAI2 in the normal adult human testis and
182 TGCTs, and IPO5 in TGCTs. The SNAI2 antibody used in this study was previously validated
183 on *Snai2* knockout mouse testis samples (7); the IPO5 antibody was previously used on adult
184 human testis and validated by Western blot using HeLa cells and adult mouse testis lysates
185 (35). SNAI2 and IPO5 antibodies were applied using a standard protocol.

186 Briefly, Bouin's fixed sections were dewaxed and rehydrated, then placed in antigen retrieval
187 solution (SNAI2 probed sections in 10 mM Citrate Buffer, pH 6.0; IPO5 probed sections in 50

188 mM Glycine, pH 3.5) for 10 minutes in a 1000W Pressure Cooker (Tefal). After cooling to
189 room temperature (RT), the sections were treated with 0.3% hydrogen peroxide for 5 minutes
190 at RT, then washed twice for 5 minutes at RT in Tris-buffered saline (TBS; 50 mM Tris, 150
191 mM NaCl, pH 7.5). Blocking solution consisted of CAS Block (Invitrogen, Thermo Fisher
192 Scientific) for 1 hr at RT in a humid chamber. Sections were incubated with anti-SNAI2
193 (Abcam, ab27568, 1:200, diluted in CAS Block) or anti-IPO5 (Santa Cruz, sc-11369, 1:1500,
194 diluted in CAS Block) overnight at RT and at 4°C, respectively, then with biotinylated anti-
195 rabbit secondary antibody (Invitrogen, #656140, 1:500, in CAS Block). Signal was amplified
196 using Vectastain Elite ABC kit reagents following the manufacturer's instructions (Vector
197 Laboratories, Burlingame, CA, USA), then a brown reaction product detected with DAB (3,3-
198 diaminobenzidine tetrahydrochloride, DAKO, Steinheim, USA). Sections were counterstained
199 using Harris haematoxylin, dehydrated and mounted using Dibutylphthalate Polystyrene
200 Xylene (DPX) (Sigma-Aldrich). Control sections lacked primary antibody to observe non-
201 specific secondary antibody binding. SNAI2 immunostaining antibody was performed on 2
202 normal adult human testes, 3 GCNIS and 3 seminoma samples, and IPO5 in 3 GCNIS and 4
203 seminoma samples.

204 **TCam-2 cell line culture**

205 The TCam-2 cell line, derived from a human seminoma (45), has been characterised as an
206 appropriate model for studies of human seminoma (46), primordial germ cells, and early
207 gonocytes (41). TCam-2 cells were maintained at 37°C (5% CO₂) in growth medium consisting
208 of RPMI 1640 medium (Gibco) containing 10% foetal calf serum (FCS; Bovogen, New
209 Zealand) with 0.5% Penicillin/Streptomycin (Pen/Strep, Gibco) and passaged at 90%
210 confluency.

211 **Immunofluorescence on fixed TCam-2 cells**

212 Immunofluorescence detection of SNAI1 and SNAI2 in TCam-2 cells was performed on cells
213 seeded in a 12 well tissue culture plate on 12 mm round glass coverslips (Menzel) at 1 x 10⁵
214 cells/well and cultured overnight. Once confluent, cells were rinsed in phosphate buffered
215 saline (PBS; Gibco), then fixed in 4% PFA for 10 minutes. Coverslips were rinsed in PBS,
216 cells permeabilised in 0.1% Triton-X 100/PBS (Merck, Darmstadt, Germany) for 10 minutes
217 and 0.5% Bovine Serum Albumin (BSA, Sigma-Aldrich)/PBS was added for 1 hour at RT to
218 block non-specific binding. Cells were incubated with primary antibodies diluted in 0.5%
219 BSA/PBS overnight at RT. Primary antibodies used were: anti-SNAI1 (Cell Signalling,

220 C15D3, 1:100) and anti-SNAI2 (Abcam, ab27568, 1:100). The following day, cells were
221 washed 3 times in PBS, then Alexa Fluor 546 goat anti-rabbit (Invitrogen, A11010, 1:500 in
222 0.5% BSA/PBS) secondary antibody was applied for 1 hr at RT. Cells were rinsed in PBS and
223 stained with 300 nM DAPI (Molecular Probes, Invitrogen) diluted in PBS for 5 minutes, rinsed
224 in PBS and mounted on slides under GVA. The specificity of the SNAI1 antibody is evident
225 from over 183 publications, including by western blot (47). The SNAI2 antibody was validated
226 as discussed above.

227 **Transfections**

228 TCam-2 cells were seeded in 6 well plates (2 X 10⁵ cells/well), then incubated overnight in
229 growth medium to reach 60% confluency. Medium was replaced with RPMI + 5% FCS,
230 lacking Pen/Strep. Transfections used the Lipofectamine™ RNAiMAX system (Invitrogen)
231 following manufacturer's instructions. Pre-designed small interfering RNAs (siRNAs)
232 (Silencer select siRNA, Thermo Fisher) were used to selectively reduce *SNAI1* (Invitrogen, 5
233 nmol, Cat #4392420, ID #s13187), *SNAI2* (Invitrogen, 5 nmol, Cat #4392420, ID # s13128),
234 and *IPO5* (Invitrogen, 5 nmol, Cat #4392420, ID S7935). Following dose-response testing, the
235 *SNAI1* siRNA construct was used at a final concentration of 25 pmol/well of 6 well plate and
236 *SNAI2* and *IPO5* siRNA constructs were used at 12.5 pmol/well. The Silencer Select Negative
237 Control siRNA *SCRAMBLE* (*SCRAM*) (Thermo Fisher, 40 nmol, Cat # 4390844) served as
238 controls in each experiment. To validate transfection efficiency, TCam-2 cells were collected
239 1 and 4 days post-transfections in TRIzol (Ambion, Life Technologies, Carlsbad, CA, USA).
240 Efficiency of gene knockdown was assessed by qRT-PCR. All experiments were independently
241 reproduced at least 3 times.

242 **Migration assay**

243 TCam-2 cells were grown to confluence in 6 well plates, then a cell free gap was generated
244 across the well using a P200 pipette tip. Growth medium was replaced with RPMI + 5% FCS
245 lacking Pen/Strep. Transfections were performed immediately after wound formation. Three
246 indicator marks per well were drawn on the plate bottom to determine specific regions of the
247 gap for subsequent imaging. Plates were photographed using a 4X objective at 0 hrs, then again
248 at 1, 2, 3, and 4 days post-gap formation to assess migration. The percentage of gap size
249 normalised to 0 hrs was determined by measuring the wound area using Image J. All
250 experiments were performed on 3 separate occasions.

251 **Viability Assay**

252 Two and three days post-transfections, TCam-2 cells were harvested using 0.1%
253 trypsin/versene (TV; 2.5% trypsin, diluted in PBS/EDTA, Gibco), rinsed in PBS and
254 resuspended in 5% FCS/PBS containing 0.05 mg/ml propidium iodide (PI, 5 mg/ml, Sigma-
255 Aldrich). The viable to non-viable cell ratio based on PI incorporation was measured on the
256 LRS-Fortessa X-20 Analyser (gated at B710-A) at the Monash University Bioplatform
257 Flowcore Facility – MHTP node. Three independent experiments were performed. The results
258 are graphed as fold-change in non-viable cells, relative to the *SCRAM* siRNA control value.
259 All experiments were repeated on 3 separate occasions.

260 **Real-time monitoring of TCam-2 cell adhesion/proliferation**

261 TCam-2 cells were seeded in 6 well plates and transfected at confluency in RPMI + 5% FCS
262 lacking Pen/Strep. One-day post-transfections, TCam-2 cells were detached using TrypLE
263 Express (Gibco) at 37°C for 5 minutes, and the reaction was quenched by adding medium. A
264 150 µl suspension of 1×10^4 cells was added to each well of an E-plate (16 wells) (ACEA
265 Biosciences, San Diego, CA). For this assay, cells were maintained in RPMI + 5% FCS. The
266 E-plate was loaded onto the xCELLigence System Real-Time Cell Analyser (RTCA; Roche)
267 in a 37°C incubator, and adhesion/proliferation measured by monitoring the impedance value
268 (Cell Index, CI) of each well every 15 minutes over 3 days. In simplest terms, the greater the
269 CI value, the greater the level of cell adhesion. Conversely, when the CI decreases, the net
270 adhesion is decreased. The cell growth rate was calculated from the slope of the line between
271 values at specific time points. Four independent experiments were performed.

272 **EdU (5-ethynyl-2'-deoxyuridine) incorporation to measure proliferation**

273 Three days post-transfection, medium was replaced with RPMI + 5% FCS containing 10 µM
274 EdU (Click-iT, EdU Flow Cytometry Assay Kit, Invitrogen). Cells were incubated at 37°C for
275 2 hrs, detached using TrypLE Express for 5 minutes and the reaction quenched. Cells were
276 pelleted, resuspended in 4% PFA/PBS, and fixed at RT for 10 minutes. After rinsing three
277 times in PBS, EdU staining was performed following the manufacturer's protocol. The ratio of
278 proliferative to non-proliferative cells, based on EdU incorporation, was measured by flow
279 cytometry (LRS-Fortessa X-20 Analyser at the Monash University Bioplatform Flowcore
280 Facility – MHTP node). Data are presented as mean values, collected in duplicate experiments.
281 Results are shown as fold-change relative to values obtained for the *SCRAM* siRNA control
282 sample.

283 **Activin A and BMP4 treatments of TCam-2 cells**

284 To determine the signalling pathways that regulate *SNAIL1* and *SNAIL2* transcripts, TCam-2 cells
285 were seeded in a 12 well plate and incubated in growth medium. Once confluent, cells were
286 serum starved (grown in RPMI alone) for 12 hrs, then treated with activin A (AA) (R&D
287 Systems Inc, Minneapolis, USA) and BMP4 (R&D Systems Inc, Minneapolis, USA), diluted
288 in RPMI only medium. A dose-response test (Fig. S3) was performed to determine the final
289 concentration of AA and BMP4 to use. TCam-2 cells were serum-starved overnight, then
290 treated with 2.5, 5, 10 and 20 ng/ml of AA or BMP4. Forty-eight hours post-treatment, TCam-2
291 cells were collected to measure *SNAIL1* and *SNAIL2* transcript levels by qRT-PCR. *SNAIL1* (Fig.
292 S3 A, B) and *SNAIL2* (Fig. S3 C, D) transcript levels reached a plateau at 5 ng/ml, suggesting
293 this as the optimal concentration of AA or BMP4 to use in this study. An equivalent volume of
294 diluent (4 mM HCl/BSA) was used as vehicle control. Forty-eight hours post-treatment, TCam-
295 2 cells were collected in TRIzol (Ambion) and Snail transcript levels were measured by qRT-
296 PCR. All experiments were repeated on 3 separate occasions. To delineate whether IPO5 is
297 required to mediate AA or BMP4 cellular responses, TCam-2 cells were seeded in a 12 well
298 plates, incubated in RPMI + 10% FCS + 0.5% Pen/Strep until 60% confluent, then transfected
299 with *SCRAM* or *IPO5* siRNAs. Twenty-four hours post-transfections, TCam-2 cells were
300 serum-starved for 12 hours, then treated with 5 ng/ml of AA or 5 ng/ml of BMP4 for 48 hours.
301 The *SCRAM* siRNA and vehicle were used as transfection and treatment controls, respectively.
302 TCam-2 cells were then collected in TRIzol (Ambion) and *SNAIL1* and *SNAIL2* transcripts were
303 measured by qRT-PCR. All experiments were repeated 3 times.

304 **Migration assay following *IPO5* or *SNAIL2* knockdown, and AA or BMP4 treatments**

305 TCam-2 cells were seeded in 6 well plates, incubated overnight until confluent and transfected
306 with 12.5 pmol of *SCRAM* and *SNAIL2* or *IPO5* siRNA constructs. Twenty-four hours post-
307 transfections, cells were serum-starved (grown in RPMI alone) for 12 hrs, then *SNAIL2*
308 transfected cells were treated with 5 ng/ml of AA or BMP4, where *IPO5* transfected TCam-2
309 cells were treated with 5 ng/ml of BMP4 only. A single scratch was generated across the well
310 and the closure of the gap size was measured over 3 days. The *SCRAM* siRNA construct and
311 vehicle were used as transfection and treatment controls, respectively. Percentage of gap size
312 normalised to 0 hrs was determined by measuring the wound area using Image J. All
313 experiments were performed on 3 separate occasions.

314 **Quantitative Real-Time PCR (qRT-PCR)**

315 Following RNA extraction using TRIzol, TCam-2 RNA samples were treated with the DNase-
316 free kit (Invitrogen Life Technologies, Oregon, USA) following the manufacturer's
317 specifications. First strand cDNA synthesis was performed with 50 μ M random hexamers
318 (Promega, Madison, WI, USA) and 10 μ M dNTPs (Sigma, St Louis, MO) for 500 ng of
319 RNA/sample. Samples were incubated at 65°C for 5 minutes to denature RNA, placed on ice,
320 then 0.1 M DTT, First Strand Buffer and Superscript III Reverse Transcriptase (Invitrogen, 200
321 U/ μ l) were added for incubation at 50°C for 1 hr. Enzymes were inactivated at 70°C for 15
322 minutes. Negative control reactions lacking Superscript III were included for each sample.
323 Quantitative Real-Time PCR was performed on the Applied Biosystems 7900HT Sequencing
324 Detection machine (Applied Biosystems, Medical Genomics Facility, Monash Health
325 Translation Precinct) at 95°C for 10 minutes, with 45 cycles of amplification at 95°C for 15
326 seconds, and 62°C for 30 seconds. Reactions were standardised against TCam-2 cDNA diluted
327 1:10, 1:40, 1:160, 1:640, 1:2560 in filtered MilliQ water. Following qRT-PCR, results were
328 analysed using the SDS Automatic Controller 2.3 (Applied Biosystems). Three independent
329 experiments were performed for each primer pair, with error bars indicating standard error of
330 the means (SEM). The sequences are listed in Table 1.

331 **Statistical analyses**

332 Values from control versus treated samples are presented as 3 or 4 independent experimental
333 results, as described in each figure legend. Mann-Whitney test, and non-parametric ANOVA
334 and Tukey's multiple comparison test were performed using GraphPad PrismTM, with $p < 0.05$
335 determining significance.

336

337 **Results**

338 **SNAI1 and SNAI2 have distinct expression profiles within the normal adult and** 339 **neoplastic human testis**

340 Our previous investigation of the postnatal mouse testis revealed that each Snail family member
341 has a distinct cellular expression profile in somatic and germline cells (7), with SNAI1 and
342 SNAI2 developmentally regulated in spermatogenic cells. We examined whether Snail
343 expression is conserved in adult human testis. In the absence of an antibody suitable for SNAI1
344 detection in paraffin embedded human tissue samples, we employed *in situ* hybridisation using
345 a validated probe and observed *SNAIL* transcript in some, but not all spermatogonia,

346 spermatocytes and peritubular cells, with a faint signal detected in Sertoli cells. Round and
347 elongated spermatids contained no detectable *SNAIL1* transcript (Fig. 1A, Fig. S1). *In situ*
348 hybridisation for detection of *SNAIL2* transcript identified a signal in spermatogonia,
349 spermatocytes, round spermatids and Sertoli cells of the normal adult human testes (Fig. 1B).
350 Further immunohistochemical analysis of normal adult human testis revealed *SNAIL2*
351 expression to be stage-specific with nuclear signal evident in some A_{dark} and A_{pale}
352 spermatogonia, late pachytene spermatocytes and round spermatids; elongated spermatids were
353 negative. Additionally, some Sertoli cell nuclei, peritubular and interstitial cells exhibited
354 *SNAIL2* immunostaining (Fig. 1C, Fig. S2). These data suggest that *SNAIL1* and *SNAIL2* are
355 active during major cellular transitions that occur during spermatogenesis and identify germ,
356 Sertoli and peritubular cells as common sites for Snail production within the normal adult
357 human testis.

358 As Snail transcription factors are central to the induction of many cancers (48-50), we further
359 investigated their expression in testicular samples containing neoplasms that retain the
360 phenotypic features of germ cells; GCNIS and seminomas. *In situ* hybridisation demonstrated
361 *SNAIL1* mRNA in some premalignant GCNIS cells (Fig. 1D, Fig S1). In seminomas, *SNAIL1* was
362 identified in seminoma cells and in the somatic cells around them (Fig. 1F, S1).
363 Immunohistochemical analysis of GCNIS samples showed strong *SNAIL2* in some GCNIS cell
364 nuclei, peritubular cells and in the extracellular matrix component (ECM) with no signal
365 evident in interstitial cells (Fig. 1E, S2 B). *SNAIL2* was detected as an intense signal in the
366 nuclei of seminoma cells in every sample (Fig. 1G, Fig. S2). Interestingly, only two of the
367 samples analysed showed nuclear *SNAIL2* within cells which resemble immune infiltrates (Fig.
368 1G, Fig. S2 D). Overall, these results indicate that *SNAIL1* and *SNAIL2* are both expressed in
369 TGCTs.

370 **The TCam-2 seminoma cell line as an *in vitro* model to assess the function of Snail proteins**

371 To delineate the role of *SNAIL1* and *SNAIL2* in TGCTs, we evaluated the suitability of using the
372 human TCam-2 seminoma cell-derived line as a model for *in vitro* analyses. We first
373 interrogated their expression in TCam-2 cells. Existing RNASeq data (51) indicates that
374 transcripts encoding *SNAIL1* and *SNAIL2*, but not *SNAIL3*, are present in TCam-2 cells (Fig. S4
375 A). This was further validated by immunofluorescence detection of nuclear *SNAIL1* and *SNAIL2*
376 protein (Fig. 2A), which is in accord with their expression in seminoma cells (Fig. 1).

377 ***SNAIL1* loss increases *SNAIL2* transcript levels**

378 To establish conditions for identifying SNAI1 and SNAI2 functions in seminoma cells, we
379 manipulated their levels in TCam-2 cells. *SNAIL1* and *SNAI2* were reduced using siRNA
380 constructs; knockdown efficiency was validated by qRT-PCR. *SNAIL1* was significantly
381 reduced following both 1 day (~ 55%) and 4 days (~ 50%) exposure to *SNAIL1* siRNA, compared
382 to *SCRAM* control sample levels (Fig 2B). *SNAI2* was significantly reduced to 70% 1 day post-
383 transfection with *SNAI2* siRNA, however there was no significant difference from *SCRAM*
384 control sample levels at 4 days (Fig 2C); this was considered as an indication that TCam-2 cells
385 lacking *SNAI2* might not be viable and was tested below. We examined the potential for SNAI1
386 and SNAI2 to compensate for each other's loss in TCam-2 cells, as described during mouse
387 chondrogenesis (52). In TCam-2 cells, lowering *SNAIL1* levels significantly increased *SNAI2* at
388 4 days post-transfection (Fig 2B), however decreased *SNAI2* did not alter *SNAIL1* (Fig 2 C).
389 This identifies a potential feedback that can occur in seminoma cells between *SNAIL1* and *SNAI2*
390 transcripts.

391 **SNAIL1 mediates cell migration and SNAI2 supports survival of TCam-2 cells**

392 To test specific potential functions of SNAI1 and SNAI2 in seminoma cells, TCam-2 behaviour
393 was assessed following siRNA-mediated transfections. We initially employed a monolayer
394 scratch assay to examine SNAI1 and SNAI2 in TCam-2 cell migration. Cells were grown in
395 5% FCS containing medium, a condition appropriate to support transfected cell growth
396 throughout the 4 day culture period, without well overgrowth. A gap was created at day 0 of
397 transfection and was measured daily. The gap size in the *SCRAM* controls reduced up to 50%
398 within 4 days. In samples with reduced *SNAIL1* levels, a significant decrease in gap closure (to
399 ~ 80% of original size) was measured (Fig. 3A), while *SNAI2* knockdown resulted in a
400 significant gap size increase between 2 and 4 days (up to ~ 125% by day 4) following
401 transfection (Fig. 3A).

402 As a gap size larger than 100% suggests cell death has occurred in the sample, TCam-2 cell
403 survival was measured by flow cytometry at 48 and 72 hrs post-transfection by propidium
404 iodide incorporation. TCam-2 cell viability was significantly decreased by *SNAI2* reduction,
405 compared to *SCRAM* control (Fig. 3B). Major contributing factors to cell death can include
406 loss of cell adhesion and cell proliferation arrest. To assess this, TCam-2 cells were transfected
407 with *SNAIL1* and *SNAI2* siRNA constructs for 24 hrs, then adhesion analysed by xCELLigence
408 every 15 minutes over 6 hours. Reduced *SNAI2* significantly decreased the proportion of
409 adherent TCam-2 cells (Fig. 3C). An initial examination by xCELLigence (Fig. 3E) suggested

410 that *SNAI2* knockdown significantly reduced the proportion of proliferating cells, however
411 further assessment by EdU incorporation identified no changes in cell proliferation when
412 measured at 72 hrs post-transfection (Fig. 3D). *SNAIL1* reduction did not affect TCam-2 cell
413 viability, adhesion or proliferation (Fig. 3 B – E).

414 ***SNAI2* transcript is elevated following stimulation with BMP4 but not activin A**

415 We investigated candidate members of the TGF- β superfamily previously linked with early
416 germline development and TGCT progression for their ability to drive expression of *SNAIL1* and
417 *SNAI2*. TCam-2 cells were treated with either activin A or BMP4 (5 ng/ml), then *SNAIL1* and
418 *SNAI2* transcripts quantified. *SNAIL1* levels were not significantly different in response to
419 activin A or BMP4 (Fig. 4A). *SNAI2* was robustly increased by BMP4 treatment, but unaffected
420 by activin A (Fig. 4B). This result identifies *SNAI2* as a selective target of BMP4 in seminoma
421 cells.

422 **IPO5, an intracellular BMP4 signalling mediator, regulates *SNAI2* expression**

423 IPO5 was recently identified to selectively transport SMADs 1/5/9 into the nucleus of human
424 liver cells to initiate BMP4-induced cellular responses (36). Immunohistochemistry identified
425 IPO5 as predominantly cytoplasmic in GCNIS and Sertoli cells (Fig. S4A-C), while
426 heterogeneous cytoplasmic and nuclear distribution of IPO5 was apparent between the different
427 seminoma samples analysed (Fig. 4C, D; Fig. S4D, E).

428 Published RNASeq data (51) showed that *IPO5* transcript levels are high in TCam-2 cell
429 samples (Fig. S4F) and was observed that the protein is readily detected by
430 immunofluorescence (data not shown). To investigate whether *SNAI2* elevation following
431 BMP4 is mediated by IPO5, an siRNA construct targeting *IPO5* was introduced and effectively
432 reduced *IPO5* levels (to < 95%, compared to *SCRAM* control levels) after 24 hrs (Fig. S4G).
433 At 24 hrs following *IPO5* knockdown, TCam-2 cells were serum-starved for 12 hrs, then
434 treated with either 5 ng/ml of activin A or BMP4. Cells were collected 48 hrs later and *SNAIL1*
435 and *SNAI2* transcript levels were quantitated. *IPO5* knockdown did not affect *SNAIL1* expression
436 following exposure to either factor (Fig. 4E), reinforcing evidence (Fig. 4A) that these
437 signalling pathways do not alter *SNAIL1* transcription. However, *IPO5* knockdown significantly
438 reduces the BMP4-mediated increase in *SNAI2* (Fig. 4F). This reveals for the first time that
439 *IPO5* levels determine the outcome of BMP4 signalling and specifically affect *SNAI2*.

440 **BMP4-induced survival of TCam-2 cells is modulated by *SNAI2***

441 BMP4 signalling pathway was shown to support TCam-2 seminoma cell survival (41). To
442 determine whether *SNAI2* contributes to BMP4-induced cellular response, we transfected
443 TCam-2 cells with the *SNAI2* siRNA constructs. Cells were serum-starved for 12 hrs, then
444 treated with 5 ng/ml of vehicle control, activin A or BMP4 for 3 days. The functional response
445 was assessed with a migration assay as described above, where a gap size larger than 100% of
446 original size indicates cell death. Vehicle (control) treatment following *SNAI2* knockdown
447 resulted in a significant increase in gap size (~ 110% of original gap size) compared to the
448 *SCRAM* control (reduced to ~ 80%) (Fig. 4G), indicating that reduced *SNAI2* levels result in
449 TCam-2 cell death, as expected and previously shown (Fig. 3 A, B). Activin A treatment of
450 TCam-2 cells following *SNAI2* knockdown resulted in gap closure (Fig. 4H); this confirms that
451 *SNAI2* is not a downstream target of activin A and suggests that activin A can support TCam-
452 2 cell migration, even when *SNAI2* is reduced. Interestingly, BMP4 treatment following *SNAI2*
453 knockdown resulted in a significant increase in gap size (~ 110%) (Fig. 4I), demonstrating that
454 BMP4 is unable to rescue the effects of *SNAI2* knockdown. These results further indicate that
455 *SNAI2* is required for BMP4-induced survival in TCam-2 cells and confirm *SNAI2* as a
456 downstream target of the BMP4 signalling pathway.

457 To determine whether *IPO5* is implicated in the signal transduction pathway proposed above,
458 TCam-2 cells were transfected with *IPO5* siRNA. Cells were serum-starved for 12 hours, then
459 treated with 5 ng/ml of the vehicle (control) or BMP4. Functional response was assessed using
460 a scratch assay, where the gap size was measured over a period of 3 days. Vehicle (control)
461 and BMP4 treatments following *IPO5* knockdown, showed a significant decrease in gap
462 closure (to ~ 95% of original gap size) compared to *SCRAM* siRNA control (Fig. 4 J, K). These
463 results suggest that reduction in *IPO5* levels did not affect BMP4-induced cell survival as
464 drastically as observed following the *SNAI2* knockdown (Fig. 4 I). As demonstrated by qRT-
465 PCR, *IPO5* knockdown significantly reduced the BMP4-induced increase in *SNAI2*, however
466 *SNAI2* transcript levels remained higher than in the vehicle control (Fig. 4F). This indicates
467 that a lower level of *SNAI2* can partially support TCam-2 cell survival.

468

469 Discussion

470 Evidence implicating Snail transcription factors in mammalian spermatogenesis is limited. The
471 current study was performed to understand how Snail factors may influence normal and
472 neoplastic germ cells in the adult human testis. It is known from *Drosophila* studies that

473 Escargot, one of the three Snail members, is expressed in the somatic hub cells, cyst stem cells
474 (CySCs) and germline stem cells (GCS) of the adult testis; its knockdown indicated that it is
475 required in hub cells to maintain niche integrity (53). A distinct profile for SNAI1 and SNAI2
476 in spermatogenic cells of the postnatal mouse testis and their co-localisation with chromatin
477 remodelling enzymes, identified their potential involvement in germ cell transitions through
478 each spermatogenic stage, where tight control of gene expression is essential (7). Aberrant
479 *Snai1* and *Snai2* levels result in germ cell loss (5, 6), implicating regulations of Snail levels are
480 important in spermatogenesis. This study demonstrates that expression profiles of SNAI1 and
481 SNAI2 in spermatogenic cells are grossly conserved between mouse and human adult testes,
482 however the heterogeneity observed in SNAI1 and 2 expression in the human testis presents
483 an interesting contrast to the more homogeneous expression in the mouse testis. Multiple
484 studies have identified considerable transcriptional heterogeneity across the spermatogonial
485 stem cell population in mammals; some examples include (54-58). These high stringency
486 single-cell level observations are increasing in frequency with more recent analyses of human
487 samples. The data presented in the current study is consistent with the single cell RNAseq data
488 in (59) study, in which human SSCs express SNAI1 and SNAI2 transcripts in around 5% of
489 SSEA4 positive SSCs (data available as GSE92276). A similarly heterogeneous expression
490 pattern in human SSCs was observed by Hermann et al 2018 (accessible at (60), “Queryable
491 single-cell RNA-seq (10x Genomics) datasets of Human and Mouse spermatogenic
492 cells”, Mendeley Data, v1<http://dx.doi.org/10.17632/kxd5f8vpt4.1>). The direct functional
493 implications of this heterogeneity are beyond the scope of the present study, but may indicate
494 there are differential roles for individual SNAIs in the 3-10 clusters of SSC subpopulations, as
495 defined by some of the studies above (reviewed in (61)). The tight regulation of SNAI
496 transcription factors in spermatogenesis is an ongoing area of interest for our lab.

497 Despite the widespread use of mice for studies examining molecular mechanisms involved in
498 testis development, spermatogenesis and the processes relating to human foetal testis growth,
499 they have significant limitations as model for human TGCT research. The absence of a mouse
500 model developing GCNIS and a seminoma-type tumours (62) restricts investigations of TGCT
501 formation and acquisition of metastatic potential to primary tissue materials and human cell
502 lines. The identification of SNAI1 and SNAI2 in TGCTs through histological analyses of
503 human samples have prompted us to examine whether they may contribute to tumour cell
504 behaviours.

505 By tightly controlling gene transcription, Snail factors promote changes in cell physiology to
506 facilitate the gain of malignant properties in several cells, including breast, gastric, colon and
507 prostate (63). Using the TCam-2 tumour cell line as an *in vitro* model, our functional studies
508 identified distinct roles for SNAI1 in facilitating migration and SNAI2 in supporting viability
509 of seminoma cells. SNAI1 was necessary for maximal TCam-2 cell migration in a wound
510 healing assay, in accordance with studies performed with prostate tumour models (64, 65).
511 SNAI2 downregulation increased TCam-2 cell death, consequently affecting their capacity to
512 adhere and migrate. The role of SNAI2 as a pro-survival factor was previously delineated
513 during development of neural crest cells (66), in gastrointestinal stromal tumour cells (67), and
514 in prostate cancer cell lines (68); in these cells, SNAI2 antagonised apoptosis through the
515 regulation of caspases or repression of pro-apoptotic markers, such as PUMA (69). Although
516 it was shown during mouse chondrogenesis that SNAI1 and SNAI2 functionally compensate
517 for each other's loss (52), their reciprocal regulation was not observed in seminoma cells. We
518 reported that by reducing *SNAI1*, *SNAI2* increased in TCam-2 cells, not *vice-versa*. This
519 resulted in survival of TCam-2 cells lacking *SNAI1*, although increased *SNAI2* levels did not
520 rescue cell migration. These outcomes reinforce the understanding that SNAI1 and SNAI2 are
521 functionally different (70) despite having highly similar protein structures (1).

522 Each Snail factor is regulated by different signalling pathways, including those mediated by
523 the TGF- β superfamily ligands (reviewed in (10)). These ligands are broadly required during
524 normal embryonic development and late stages of tumorigenesis, where TGF- β activation
525 upregulates Snail factors to promote EMT (71). Phosphorylated SMADs and transcripts
526 encoding ACVR1A, ACVR1B, BMPR1A and BMPR2 are detectable within seminomas (38),
527 indicating that TGF- β signalling is active. Primary cultures of seminoma testis fragments
528 responded to activin A, resulting in a decrease in *KIT* mRNA and protein (72). TCam-2 cell
529 exposure to activin A or to BMP4 promoted proliferation or survival, respectively (41),
530 suggesting that TGF- β superfamily signalling activity can influence seminoma progression.
531 Here we showed that *SNAI2*, but not *SNAI1*, dramatically increased in TCam-2 cells following
532 exposure to BMP4 for 48 hrs (Fig. 4), revealing *SNAI2* as a BMP4 downstream target. To
533 reinforce this, we selectively manipulated the BMP4 signalling pathway by knockdown of
534 IPO5, and thereby drastically reduced the capacity for BMP4 exposure to elevate *SNAI2*. These
535 new findings extend our previous report that showed BMP4 supports TCam-2 cell survival (41)
536 by revealing *SNAI2* as a BMP4 downstream target that mediates BMP4-induced survival in
537 seminoma cells. The variable distribution of IPO5 between the cytoplasm and nucleus, present

538 in individual seminoma cells suggests this may indicate different levels of BMP4 signalling;
539 cytoplasmic IPO5 would be expected to perform the canonical nucleocytoplasmic transport
540 role of shuttling transcription factors into the nucleus (73-75), whereas nuclear IPO5 has been
541 shown to indirectly modulate gene transcription (76). Despite a previous report that activin A
542 increases *SNAI2* during placental development (43), it did not regulate Snail levels in TCam-2
543 cells. More remains to be learned about the fine-tuning of TGF- β signalling in TGCTs,
544 including how they interact to effect transcription of different downstream targets.

545 The novel observations from this study provide evidence that *SNAI1* and *SNAI2* are important
546 for both normal and neoplastic germ cell functions. Their concurrent expression in seminoma
547 cells indicate that *SNAI1* and *SNAI2* may support the induction and maintenance of the tumour
548 phenotype. In conclusion, we propose that minimising *SNAI2*, but not *SNAI1*, levels repress
549 BMP4-induced survival of seminoma cells, suggesting that *SNAI2* is a potential therapeutic
550 target.

551 **Acknowledgments:** The authors would like to thank Dr. Maciej Szarek for technical support,
552 Sarah Moody for provision of materials, and Dr. Liza O'Donnell for expert advice on germ cell
553 identification in the normal adult human testis.

554 **Author Contributions:**

555 Diana J. Micati: Study conception and design, experimental data acquisition, analysis and
556 interpretation, manuscript writing, manuscript revision, final manuscript approval.

557 Karthika Radhakrishnan: experimental data acquisition, manuscript revision and final
558 manuscript approval.

559 Julia C. Young: Study design, data analysis and interpretation, manuscript revision and final
560 manuscript approval.

561 Ewa Rajpert-De Meyts: provision of key materials, manuscript revision and final manuscript
562 approval.

563 Gary R. Hime: Study conception and design, experimental analysis and data interpretation,
564 manuscript revision, final manuscript approval.

565 Helen E. Abud: Study conception and design, experimental analysis and data interpretation,
566 manuscript revision, final manuscript approval.

567 Kate L. Loveland: Study conception and design, experimental analysis and data interpretation,
568 manuscript writing and revision, final manuscript approval.

569 **Compliance with ethical standards:** All procedures involving normal adult human testis and
570 TGCT samples were approved by the Monash University Human Research Ethics Committee
571 and the Regional Committee for Medical Research Ethics (Copenhagen), respectively.

572 **Conflict of interest:** The authors have no conflicts of interest in presenting information and
573 material described in this paper.

574 **References**

- 575 1. Nieto MA. The snail superfamily of zinc-finger transcription factors. *Nature reviews*
576 *Molecular cell biology*. 2002;3(3):155-66.
- 577 2. Lin Y, Dong C, Zhou BP. Epigenetic regulation of EMT: the Snail story. *Current pharmaceutical*
578 *design*. 2014;20(11):1698-705.
- 579 3. Kataoka H, Murayama T, Yokode M, Mori S, Sano H, Ozaki H, et al. A novel snail-related
580 transcription factor Smuc regulates basic helix-loop-helix transcription factor activities via specific E-
581 box motifs. *Nucleic acids research*. 2000;28(2):626-33.
- 582 4. Chiang C, Ayyanathan K. Snail/Gfi-1 (SNAG) family zinc finger proteins in transcription
583 regulation, chromatin dynamics, cell signaling, development, and disease. *Cytokine & growth factor*
584 *reviews*. 2013;24(2):123-31.
- 585 5. Kanarek N, Horwitz E, Mayan I, Leshets M, Cojocaru G, Davis M, et al. Spermatogenesis
586 rescue in a mouse deficient for the ubiquitin ligase SCF{beta}-TrCP by single substrate depletion.
587 *Genes & development*. 2010;24(5):470-7.
- 588 6. Perez-Losada J, Sanchez-Martin M, Rodriguez-Garcia A, Sanchez ML, Orfao A, Flores T, et al.
589 Zinc-finger transcription factor Slug contributes to the function of the stem cell factor c-kit signaling
590 pathway. *Blood*. 2002;100(4):1274-86.
- 591 7. Micati DJ, Hime GR, McLaughlin EA, Abud HE, Loveland KL. Differential expression profiles of
592 conserved Snail transcription factors in the mouse testis. *Andrology*. 2018;6(2):362-73.
- 593 8. Mu W, Starmer J, Fedoriw AM, Yee D, Magnuson T. Repression of the soma-specific
594 transcriptome by Polycomb-repressive complex 2 promotes male germ cell development. *Genes &*
595 *development*. 2014;28(18):2056-69.
- 596 9. Myrick DA, Christopher MA, Scott AM, Simon AK, Donlin-Asp PG, Kelly WG, et al.
597 KDM1A/LSD1 regulates the differentiation and maintenance of spermatogonia in mice. *PLoS one*.
598 2017;12(5):e0177473.
- 599 10. Wu Y, Zhou BP. Snail: More than EMT. *Cell Adh Migr*. 2010;4(2):199-203.

- 600 11. Wang Y, Shi J, Chai K, Ying X, Zhou BP. The Role of Snail in EMT and Tumorigenesis. *Current*
601 *cancer drug targets*. 2013;13(9):963-72.
- 602 12. Batlle E, Sancho E, Franci C, Dominguez D, Monfar M, Baulida J, et al. The transcription factor
603 snail is a repressor of E-cadherin gene expression in epithelial tumour cells. *Nature cell biology*.
604 2000;2(2):84-9.
- 605 13. Horvay K, Jarde T, Casagrande F, Perreau VM, Haigh K, Nefzger CM, et al. Snai1 regulates cell
606 lineage allocation and stem cell maintenance in the mouse intestinal epithelium. *The EMBO journal*.
607 2015;34(10):1319-35.
- 608 14. Horvay K, Casagrande F, Gany A, Hime GR, Abud HE. Wnt signaling regulates Snai1
609 expression and cellular localization in the mouse intestinal epithelial stem cell niche. *Stem Cells Dev*.
610 2011;20(4):737-45.
- 611 15. Chen YC, Chen YW, Hsu HS, Tseng LM, Huang PI, Lu KH, et al. Aldehyde dehydrogenase 1 is a
612 putative marker for cancer stem cells in head and neck squamous cancer. *Biochem Biophys Res*
613 *Commun*. 2009;385(3):307-13.
- 614 16. Zhou W, Lv R, Qi W, Wu D, Xu Y, Liu W, et al. Snail contributes to the maintenance of stem
615 cell-like phenotype cells in human pancreatic cancer. *PloS one*. 2014;9(1):e87409.
- 616 17. Jones RJ, Matsui WH, Smith BD. Cancer stem cells: are we missing the target? *J Natl Cancer*
617 *Inst*. 2004;96(8):583-5.
- 618 18. Yang HW, Menon LG, Black PM, Carroll RS, Johnson MD. SNAI2/Slug promotes growth and
619 invasion in human gliomas. *BMC Cancer*. 2010;10:301.
- 620 19. Kim S, Yao J, Suyama K, Qian X, Qian BZ, Bandyopadhyay S, et al. Slug promotes survival
621 during metastasis through suppression of Puma-mediated apoptosis. *Cancer research*.
622 2014;74(14):3695-706.
- 623 20. Skakkebaek NE. Abnormal morphology of germ cells in two infertile men. *Acta Pathol*
624 *Microbiol Scand A*. 1972;80(3):374-8.
- 625 21. Rajpert-De Meyts E. Developmental model for the pathogenesis of testicular carcinoma in
626 situ: genetic and environmental aspects. *Hum Reprod Update*. 2006;12(3):303-23.
- 627 22. Looijenga LH, Gillis AJ, Stoop H, Biermann K, Oosterhuis JW. Dissecting the molecular
628 pathways of (testicular) germ cell tumour pathogenesis; from initiation to treatment-resistance.
629 *International journal of andrology*. 2011;34(4 Pt 2):e234-51.
- 630 23. Ulbright TM. Germ cell neoplasms of the testis. *Am J Surg Pathol*. 1993;17(11):1075-91.
- 631 24. Ferlay J, Soerjomataram I, Dikshit R, Eser S, Mathers C, Rebelo M, et al. Cancer incidence and
632 mortality worldwide: sources, methods and major patterns in GLOBOCAN 2012. *Int J Cancer*.
633 2015;136(5):E359-86.

- 634 25. Williamson SR, Delahunt B, Magi-Galluzzi C, Algaba F, Egevad L, Ulbright TM, et al. The World
635 Health Organization 2016 classification of testicular germ cell tumours: a review and update from
636 the International Society of Urological Pathology Testis Consultation Panel. *Histopathology*.
637 2017;70(3):335-46.
- 638 26. Itman C, Wong C, Whiley PA, Fernando D, Loveland KL. TGFbeta superfamily signaling
639 regulators are differentially expressed in the developing and adult mouse testis. *Spermatogenesis*.
640 2011;1(1):63-72.
- 641 27. Le Bras GF, Loomans HA, Taylor CJ, Revetta FL, Andl CD. Activin A balance regulates epithelial
642 invasiveness and tumorigenesis. *Lab Invest*. 2014;94(10):1134-46.
- 643 28. Alarmo EL, Huhtala H, Korhonen T, Pylkkanen L, Holli K, Kuukasjarvi T, et al. Bone
644 morphogenetic protein 4 expression in multiple normal and tumor tissues reveals its importance
645 beyond development. *Mod Pathol*. 2013;26(1):10-21.
- 646 29. Wang RN, Green J, Wang Z, Deng Y, Qiao M, Peabody M, et al. Bone Morphogenetic Protein
647 (BMP) signaling in development and human diseases. *Genes Dis*. 2014;1(1):87-105.
- 648 30. Hill CS. Transcriptional Control by the SMADs. *Cold Spring Harb Perspect Biol*. 2016;8(10).
- 649 31. Tsuchida K, Nakatani M, Hitachi K, Uezumi A, Sunada Y, Ageta H, et al. Activin signaling as an
650 emerging target for therapeutic interventions. *Cell Commun Signal*. 2009;7:15.
- 651 32. Loveland KL, Major AT, Butler R, Young JC, Jans DA, Miyamoto Y. Putting things in place for
652 fertilization: discovering roles for importin proteins in cell fate and spermatogenesis. *Asian J Androl*.
653 2015;17(4):537-44.
- 654 33. Hogarth C, Itman C, Jans DA, Loveland KL. Regulated nucleocytoplasmic transport in
655 spermatogenesis: a driver of cellular differentiation? *Bioessays*. 2005;27(10):1011-25.
- 656 34. Hogarth CA, Jans DA, Loveland KL. Subcellular distribution of importins correlates with germ
657 cell maturation. *Dev Dyn*. 2007;236(8):2311-20.
- 658 35. Whiley PA, Miyamoto Y, McLachlan RI, Jans DA, Loveland KL. Changing subcellular
659 localization of nuclear transport factors during human spermatogenesis. *International journal of*
660 *andrology*. 2012;35(2):158-69.
- 661 36. Baas R, Sijm A, van Teeffelen HA, van Es R, Vos HR, Marc Timmers HT. Quantitative
662 Proteomics of the SMAD (Suppressor of Mothers against Decapentaplegic) Transcription Factor
663 Family Identifies Importin 5 as a Bone Morphogenic Protein Receptor SMAD-specific Importin. *The*
664 *Journal of biological chemistry*. 2016;291(46):24121-32.
- 665 37. Dias V, Meachem S, Rajpert-De Meyts E, McLachlan R, Manuelpillai U, Loveland KL. Activin
666 receptor subunits in normal and dysfunctional adult human testis. *Hum Reprod*. 2008;23(2):412-20.

- 667 38. Dias VL, Rajpert-De Meyts E, McLachlan R, Loveland KL. Analysis of activin/TGFB-signaling
668 modulators within the normal and dysfunctional adult human testis reveals evidence of altered
669 signaling capacity in a subset of seminomas. *Reproduction*. 2009;138(5):801-11.
- 670 39. Fustino N, Rakheja D, Ateek CS, Neumann JC, Amatruda JF. Bone morphogenetic protein
671 signalling activity distinguishes histological subsets of paediatric germ cell tumours. *International*
672 *journal of andrology*. 2011;34(4 Pt 2):e218-33.
- 673 40. Neumann JC, Chandler GL, Damoulis VA, Fustino NJ, Lillard K, Looijenga L, et al. Mutation in
674 the type IB bone morphogenetic protein receptor Alk6b impairs germ-cell differentiation and causes
675 germ-cell tumors in zebrafish. *Proceedings of the National Academy of Sciences of the United States*
676 *of America*. 2011;108(32):13153-8.
- 677 41. Young JC, Jaiprakash A, Mithraprabhu S, Itman C, Kitazawa R, Looijenga LH, et al. TCam-2
678 seminoma cell line exhibits characteristic foetal germ cell responses to TGF-beta ligands and retinoic
679 acid. *International journal of andrology*. 2011;34(4 Pt 2):e204-17.
- 680 42. Sonne SB, Almstrup K, Dalgaard M, Juncker AS, Edsgard D, Ruban L, et al. Analysis of gene
681 expression profiles of microdissected cell populations indicates that testicular carcinoma in situ is an
682 arrested gonocyte. *Cancer research*. 2009;69(12):5241-50.
- 683 43. Li Y, Klausen C, Zhu H, Leung PC. Activin A Increases Human Trophoblast Invasion by Inducing
684 SNAIL-Mediated MMP2 Up-Regulation Through ALK4. *J Clin Endocrinol Metab*. 2015;100(11):E1415-
685 27.
- 686 44. Kestens C, Siersema PD, Offerhaus GJ, van Baal JW. Correction: BMP4 Signaling Is Able to
687 Induce an Epithelial-Mesenchymal Transition-Like Phenotype in Barrett's Esophagus and Esophageal
688 Adenocarcinoma through Induction of SNAIL2. *PloS one*. 2016;11(6):e0158755.
- 689 45. Mizuno Y, Gotoh A, Kamidono S, Kitazawa S. [Establishment and characterization of a new
690 human testicular germ cell tumor cell line (TCam-2)]. *Nihon Hinyokika Gakkai Zasshi*.
691 1993;84(7):1211-8.
- 692 46. de Jong J, Stoop H, Gillis AJ, Hersmus R, van Gurp RJ, van de Geijn GJ, et al. Further
693 characterization of the first seminoma cell line TCam-2. *Genes Chromosomes Cancer*.
694 2008;47(3):185-96.
- 695 47. Chang KK, Yoon C, Yi BC, Tap WD, Simon MC, Yoon SS. Platelet-derived growth factor
696 receptor-alpha and -beta promote cancer stem cell phenotypes in sarcomas. *Oncogenesis*.
697 2018;7(6):47.
- 698 48. De Craene B, Denecker G, Vermassen P, Taminau J, Mauch C, Derore A, et al. Epidermal Snail
699 expression drives skin cancer initiation and progression through enhanced cytoprotection, epidermal

700 stem/progenitor cell expansion and enhanced metastatic potential. *Cell Death Differ.*
701 2014;21(2):310-20.

702 49. Lu ZY, Dong R, Li D, Li WB, Xu FQ, Geng Y, et al. SNAIL1 overexpression induces stemness and
703 promotes ovarian cancer cell invasion and metastasis. *Oncology reports.* 2012;27(5):1587-91.

704 50. Hwang WL, Yang MH, Tsai ML, Lan HY, Su SH, Chang SC, et al. SNAIL regulates interleukin-8
705 expression, stem cell-like activity, and tumorigenicity of human colorectal carcinoma cells.
706 *Gastroenterology.* 2011;141(1):279-91, 91 e1-5.

707 51. Kim S, Gunesdogan U, Zyllicz JJ, Hackett JA, Cougot D, Bao S, et al. PRMT5 protects genomic
708 integrity during global DNA demethylation in primordial germ cells and preimplantation embryos.
709 *Molecular cell.* 2014;56(4):564-79.

710 52. Chen Y, Gridley T. Compensatory regulation of the Snai1 and Snai2 genes during
711 chondrogenesis. *Journal of bone and mineral research : the official journal of the American Society*
712 *for Bone and Mineral Research.* 2013;28(6):1412-21.

713 53. Voog J, Sandall SL, Hime GR, Resende LP, Loza-Coll M, Aslanian A, et al. Escargot restricts
714 niche cell to stem cell conversion in the Drosophila testis. *Cell Rep.* 2014;7(3):722-34.

715 54. Hammoud SS, Low DH, Yi C, Carrell DT, Guccione E, Cairns BR. Chromatin and transcription
716 transitions of mammalian adult germline stem cells and spermatogenesis. *Cell stem cell.*
717 2014;15(2):239-53.

718 55. Hammoud SS, Low DH, Yi C, Lee CL, Oatley JM, Payne CJ, et al. Transcription and imprinting
719 dynamics in developing postnatal male germline stem cells. *Genes & development.*
720 2015;29(21):2312-24.

721 56. Kanatsu-Shinohara M, Shinohara T. Spermatogonial stem cell self-renewal and development.
722 *Annu Rev Cell Dev Biol.* 2013;29:163-87.

723 57. La HM, Makela JA, Chan AL, Rossello FJ, Nefzger CM, Legrand JMD, et al. Identification of
724 dynamic undifferentiated cell states within the male germline. *Nat Commun.* 2018;9(1):2819.

725 58. von Kopylow K, Schulze W, Salzbrunn A, Spiess AN. Isolation and gene expression analysis of
726 single potential human spermatogonial stem cells. *Molecular human reproduction.* 2016;22(4):229-
727 39.

728 59. Guo J, Grow EJ, Yi C, Mlcochova H, Maher GJ, Lindskog C, et al. Chromatin and Single-Cell
729 RNA-Seq Profiling Reveal Dynamic Signaling and Metabolic Transitions during Human
730 Spermatogonial Stem Cell Development. *Cell stem cell.* 2017;21(4):533-46 e6.

731 60. Hermann BP, Cheng K, Singh A, Roa-De La Cruz L, Mutoji KN, Chen IC, et al. The Mammalian
732 Spermatogenesis Single-Cell Transcriptome, from Spermatogonial Stem Cells to Spermatids. *Cell Rep.*
733 2018;25(6):1650-67 e8.

- 734 61. Tan K, Wilkinson MF. Human Spermatogonial Stem Cells Scrutinized under the Single-Cell
735 Magnifying Glass. *Cell stem cell*. 2019;24(2):201-3.
- 736 62. Zechel JL, MacLennan GT, Heaney JD, Nadeau JH. Spontaneous metastasis in mouse models
737 of testicular germ-cell tumours. *International journal of andrology*. 2011;34(4 Pt 2):e278-87.
- 738 63. Kaufhold S, Bonavida B. Central role of Snail1 in the regulation of EMT and resistance in
739 cancer: a target for therapeutic intervention. *Journal of experimental & clinical cancer research : CR*.
740 2014;33:62.
- 741 64. Li H, Li M, Xu D, Zhao C, Liu G, Wang F. Overexpression of Snail in retinal pigment epithelial
742 triggered epithelial-mesenchymal transition. *Biochem Biophys Res Commun*. 2014;446(1):347-51.
- 743 65. Osorio LA, Farfan NM, Castellon EA, Contreras HR. SNAIL transcription factor increases the
744 motility and invasive capacity of prostate cancer cells. *Mol Med Rep*. 2016;13(1):778-86.
- 745 66. Tribulo C, Aybar MJ, Sanchez SS, Mayor R. A balance between the anti-apoptotic activity of
746 Slug and the apoptotic activity of msx1 is required for the proper development of the neural crest.
747 *Developmental biology*. 2004;275(2):325-42.
- 748 67. Pulkka OP, Nilsson B, Sarlomo-Rikala M, Reichardt P, Eriksson M, Hall KS, et al. SLUG
749 transcription factor: a pro-survival and prognostic factor in gastrointestinal stromal tumour. *British
750 journal of cancer*. 2017;116(9):1195-202.
- 751 68. Emadi Baygi M, Soheili ZS, Essmann F, Deezagi A, Engers R, Goering W, et al. Slug/SNAI2
752 regulates cell proliferation and invasiveness of metastatic prostate cancer cell lines. *Tumour Biol*.
753 2010;31(4):297-307.
- 754 69. Wu WS, Heinrichs S, Xu D, Garrison SP, Zambetti GP, Adams JM, et al. Slug antagonizes p53-
755 mediated apoptosis of hematopoietic progenitors by repressing puma. *Cell*. 2005;123(4):641-53.
- 756 70. Villarejo A, Cortes-Cabrera A, Molina-Ortiz P, Portillo F, Cano A. Differential role of Snail1 and
757 Snail2 zinc fingers in E-cadherin repression and epithelial to mesenchymal transition. *The Journal of
758 biological chemistry*. 2014;289(2):930-41.
- 759 71. Saitoh M, Miyazawa K. Transcriptional and post-transcriptional regulation in TGF-beta-
760 mediated epithelial-mesenchymal transition. *J Biochem*. 2012;151(6):563-71.
- 761 72. Jorgensen A, Young J, Nielsen JE, Joensen UN, Toft BG, Rajpert-De Meyts E, et al. Hanging
762 drop cultures of human testis and testis cancer samples: a model used to investigate activin
763 treatment effects in a preserved niche. *British journal of cancer*. 2014;110(10):2604-14.
- 764 73. Nakatani T, Yamagata K, Kimura T, Oda M, Nakashima H, Hori M, et al. Stella preserves
765 maternal chromosome integrity by inhibiting 5hmC-induced gammaH2AX accumulation. *EMBO Rep*.
766 2015;16(5):582-9.

- 767 74. Heese K, Yamada T, Akatsu H, Yamamoto T, Kosaka K, Nagai Y, et al. Characterizing the new
768 transcription regulator protein p60TRP. *J Cell Biochem.* 2004;91(5):1030-42.
- 769 75. Swale C, Monod A, Tengo L, Labaronne A, Garzoni F, Bourhis JM, et al. Structural
770 characterization of recombinant IAV polymerase reveals a stable complex between viral PA-PB1
771 heterodimer and host RanBP5. *Sci Rep.* 2016;6:24727.
- 772 76. Clerman A, Noor Z, Fischelevich R, Lockatell V, Hampton BS, Shah NG, et al. The full-length
773 interleukin-33 (IL33)-importin-5 interaction does not regulate nuclear localization of IL33 but
774 controls its intracellular degradation. *The Journal of biological chemistry.* 2017;292(52):21653-61.

775

776 **Figures**

777 **Figure SNAI1 and SNAI2 are present in normal and neoplastic human testis samples.**

778 *In situ* hybridisation with *SNAI1* antisense cRNA probe detected *SNAI1* transcript in normal
779 adult human testis (A), GCNIS (D), and seminoma (F) samples. Immunocytochemical staining
780 revealed *SNAI2* mRNA (B) and protein (C) in the normal adult human testis, and SNAI2
781 protein in GCNIS (E) and seminoma (G) samples. Primary antibody was omitted in negative
782 control (insert). Blue arrow = spermatogonia; green arrow = spermatocytes; white arrow =
783 spermatids; grey arrow = Sertoli cells; red arrow = peritubular cells; yellow arrow = interstitial
784 cells; purple arrow = GCNIS cells; orange arrow = seminoma cells; pink arrow = immune cell
785 infiltrates. Scale bar = 10 μ m.

786

787 **Figure 2 SNAI1 and SNAI2 in TCam-2 cells, and evidence of reciprocal expression.** (A)
788 Immunofluorescence identified SNAI1 and SNAI2 in TCam-2 cell nuclei. Scale bar = 10 μ m.
789 (B, C) siRNA knockdown of *SNAI1* (B) and *SNAI2* (C). Knockdown efficiency and
790 *SNAI1/SNAI2* reciprocal regulation were each documented at 1 (t 1) and 4 (t 4) days post-
791 transfections. The SCRAM siRNA construct served as transfection control. Graphs are
792 presented as mean values, with error bars representing SEM, and significance was determined
793 using the Mann-Whitney test. * $p < 0.05$, $n = 3$.

794

795 **Figure 3 SNAI1 and SNAI2 differentially affect TCam-2 cell behaviour.** TCam-2 cells were
796 transfected with *SNAI1*, *SNAI2* and *SCRAM* siRNA constructs to measure: (A) migration, (B)
797 viability, (C) adhesion, and proliferation by BrdU incorporation (D) and xCELLigence real-time

798 analysis (E). Graphs present mean values, with error bars representing the SEM. For viability,
799 adhesion and proliferation assays, significance was determined using the Mann-Whitney test,
800 * $p < 0.05$. For migration, non-parametric ANOVA and Tukey's multiple comparison test
801 determined significance, * $p < 0.05$.

802

803 **Figure 4 BMP4-induced survival and migration of TCam-2 cells is reduced by SNAI2**
804 **inhibition.** (A, B) Changes in *SNAI1* and *SNAI2* transcript levels following activin A (AA) and
805 BMP4 treatments were assessed by qRT-PCR. (C, D) Immunohistochemical analysis revealed
806 that IPO5 subcellular localisation was heterogenous in seminomas ($n = 4$). Primary antibody
807 was omitted in negative controls (inserts; c, d). Scale bar = 10 μm . (E, F) TCam-2 cells
808 transfected with *IPO5* siRNA construct were treated with vehicle control, AA or BMP4, then
809 *SNAI1* and *SNAI2* levels were measured by qRT-PCR. *Sc* siRNA and vehicle were used as
810 transfection and treatment controls, respectively. Each value was normalised to *RPLP0*. Graphs
811 present mean values; error bars indicate SEM. Statistical analysis was performed relative to the
812 vehicle control. Significance was calculated using the Mann-Whitney test, * $p < 0.05$. (G - I)
813 TCam-2 cells transfected with *SNAI2* (G-I) or *IPO5* (J, K) siRNA constructs were treated with
814 vehicle control, AA or BMP4, then effects on migration were measured. Wound area is
815 presented relative to the gap measured at time point 0. *Sc* siRNA and vehicle were used as
816 transfection and treatment controls, respectively. Graphs are presented as mean values, with
817 error bars indicating SEM, and significance was determined through 2-way Anova. * $p < 0.05$,
818 $n = 3$.

819

820 **Fig. S1. Expression of *SNAI1* transcript in the normal adult and neoplastic human testis.**
821 Purple staining indicates the cellular sites of *SNAI1* mRNA synthesis in the additional normal
822 adult (A) and neoplastic human testis (B – E) samples. Within the second normal adult human
823 testis sample Blue arrow = spermatogonia; green arrow = spermatocytes; grey arrow = Sertoli
824 cells; red arrow = peritubular cells; yellow arrow = interstitial cells; purple arrow = GCNIS
825 cells; orange arrow = seminoma cells; pink arrow = immune cell infiltrates. Scale bar = 10 μm .

826 **Fig. S2. *SNAI2* localisation in the normal adult and neoplastic human testis.** Brown
827 staining indicates *SNAI2* protein localisation in the normal adult human testis (A), GCNIS (B,
828 C), and seminoma (D, E) samples. Intense background signal is evident within the interstitium
829 of the normal adult human and GCNIS testis samples. Blue arrow = spermatogonia; green

830 arrow = spermatocytes; white arrow = spermatids; grey arrow = Sertoli cells; red arrow =
831 peritubular cells; yellow arrow = interstitial cells; purple arrow = GCNIS cells; orange arrow
832 = seminoma cells; pink arrow = immune cell infiltrates. Scale bar = 10 μ m.

833

834 **Fig. S3. Dose-response of activin A and BMP4 on Snail transcript levels.** Serum-starved
835 TCam-2 cells were treated with increasing dose of activin A and BMP4. Forty-eight hours post-
836 treatment, *SNAIL1* (A, B) and *SNAIL2* (C, D) transcript levels were measured. Graphs show the
837 mean values. These experiments were repeated twice.

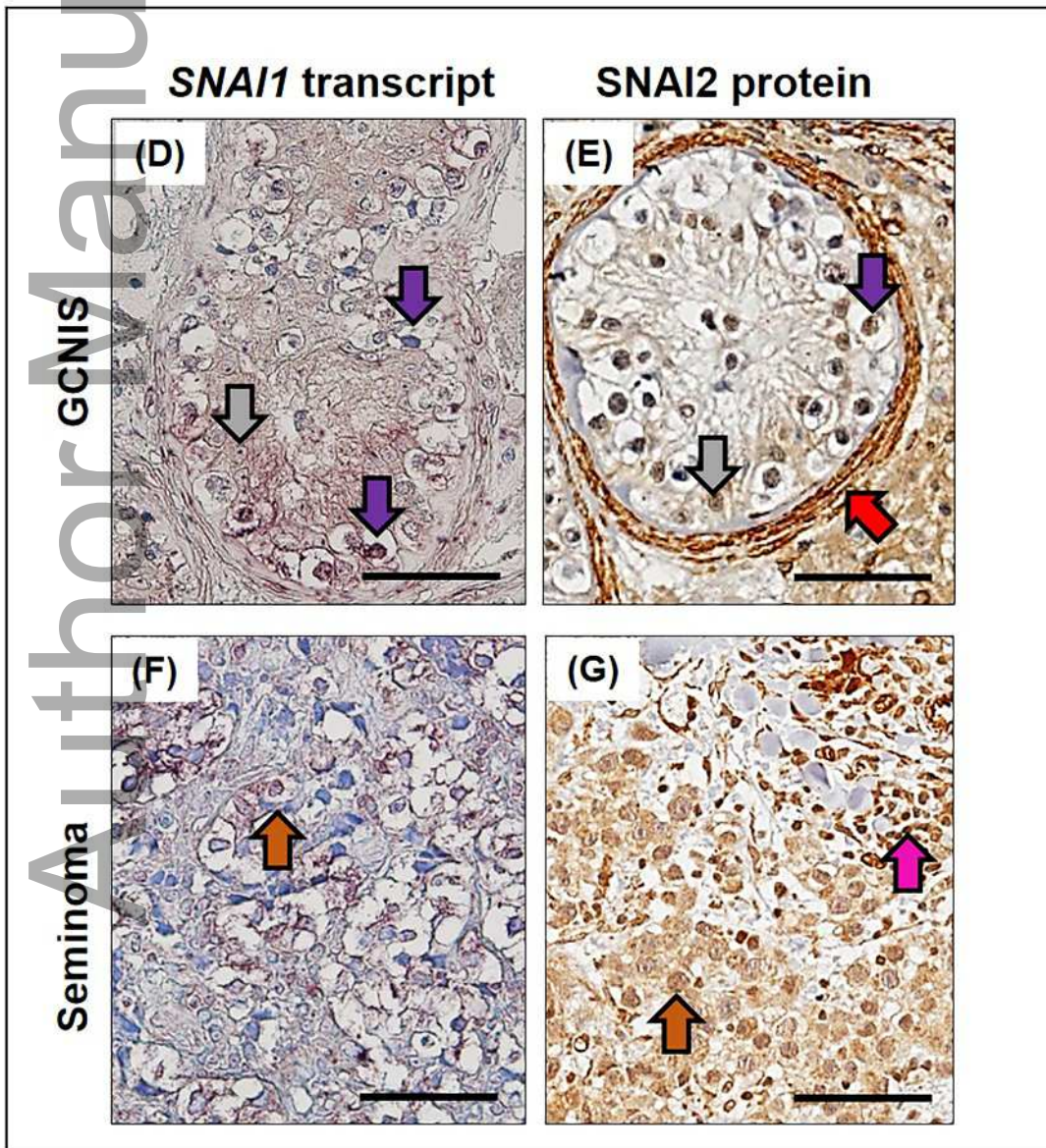
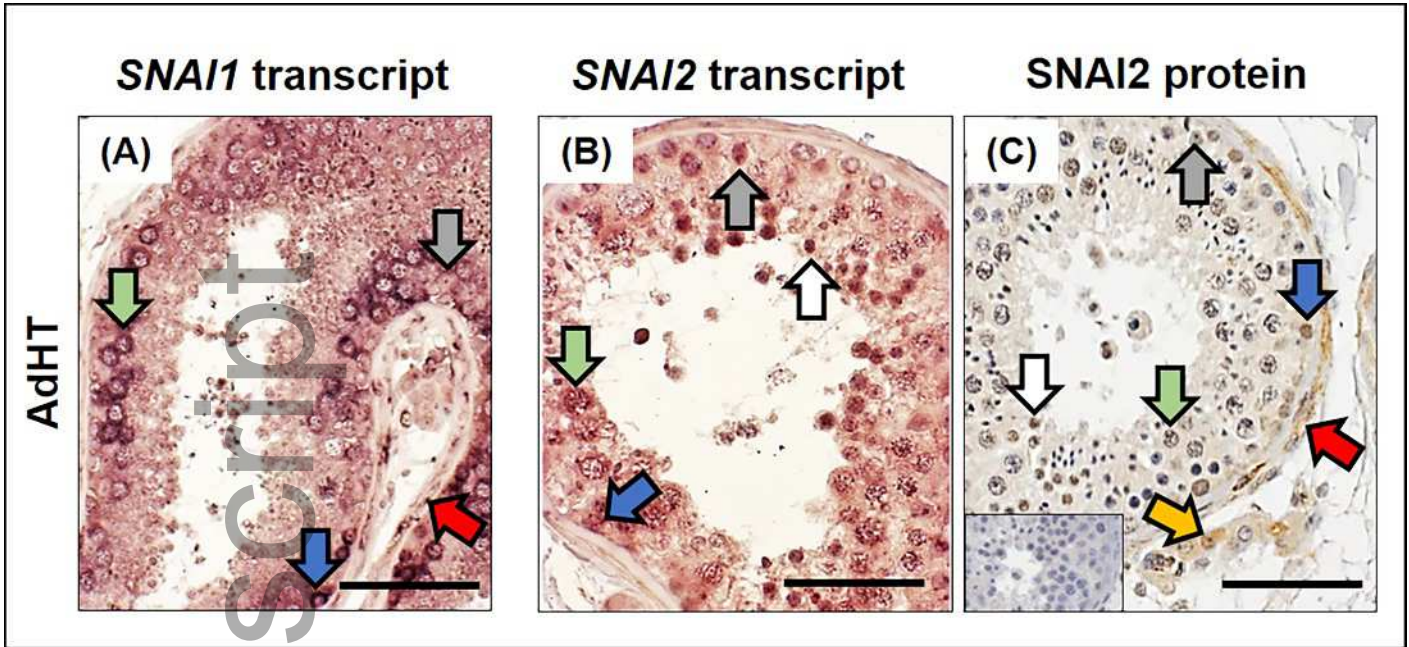
838

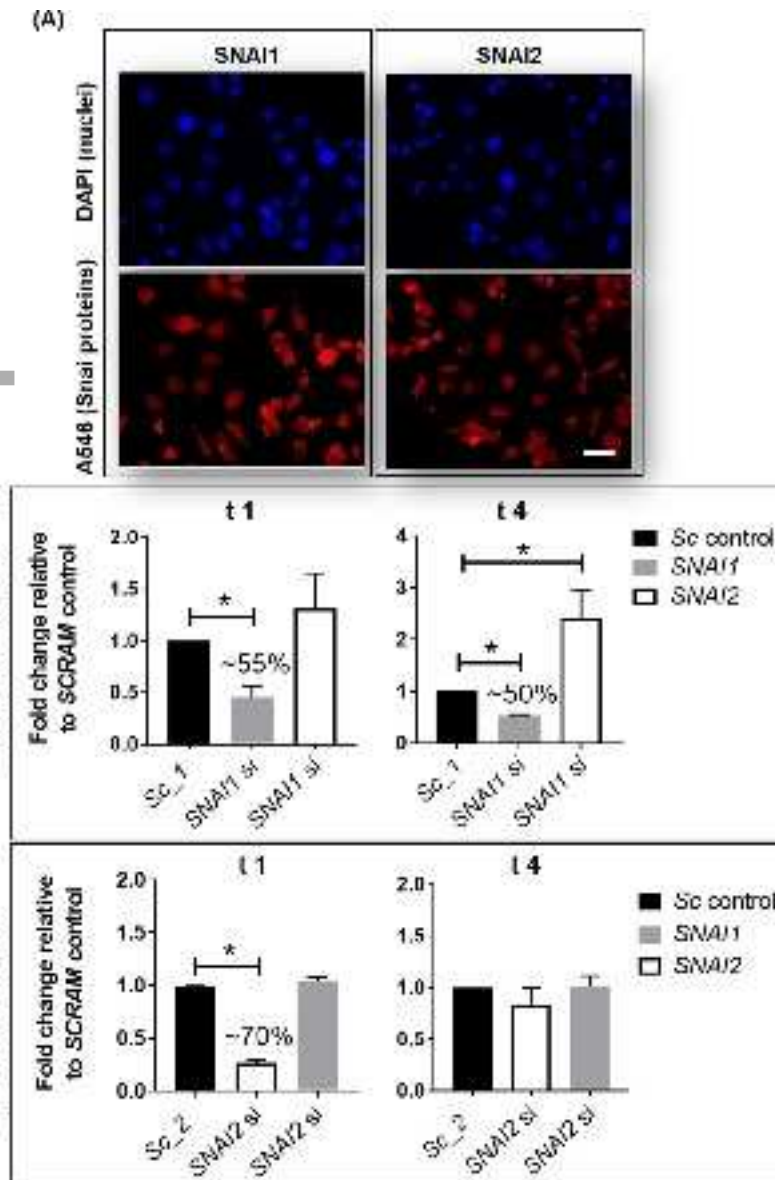
839 **Fig. S4 IPO5 protein localisation in TGCT samples, and IPO5 and Snail expression in**
840 **TCam-2 cells. (A - E) IPO5 subcellular localisation** in GCNIS (A - C) and seminoma (D, E)
841 samples was heterogeneous. **(F) SNAIL1, SNAIL2, SNAIL3 and IPO5 were measured in two**
842 **TCam-2 cell samples.** The Surani RNASeq demonstrated that *SNAIL1*, *SNAIL2* and *IPO5*, not
843 *SNAIL3*, are detectable in TCam-2 cells. **(G) IPO5 knockdown in TCam-2 cells.** TCam-2 cells
844 were transfected for 24 hrs with 12.5 pmol of *SCRAM* control and *IPO5* siRNA constructs,
845 then treated with 5 ng/ml of vehicle control, AA or BMP4. Knockdown efficiency was
846 measured 48 hrs post-treatment. Graphs show mean values, with error bars representing SEM.
847 Significance was determined using the Mann-Whitney test. * $p < 0.05$, $n = 3$. Purple arrow =
848 GCNIS cells; grey arrow = Sertoli cells; orange arrow = seminoma cells. Scale bars = 10 μ m.

Author Manuscript

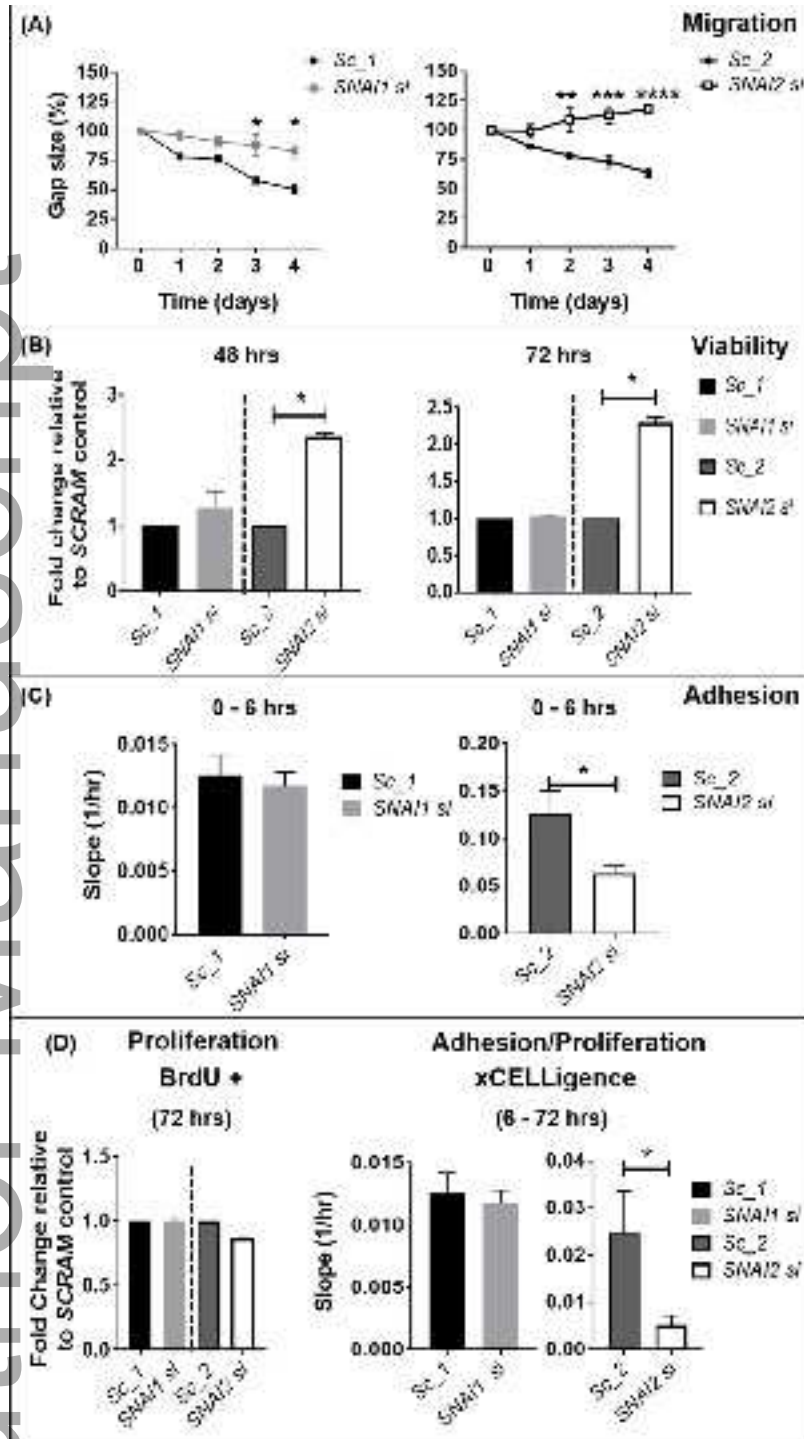
Gene	Accession number	Forward (5'-3')	Reverse (5'-3')	Technique
SNAI1	NM_005985	CTGCGTGGGTTTTGTATCC	TCGGGGCATCTCAGACTCTA	<i>in situ</i> hybridisation
SNAI2	NM_003068	GAGAGCTGCAAGAGCATGGA	TTGCTGCCAAATCATTTC	<i>in situ</i> hybridisation
RPLP0	NM_001002	CTATCATCAACGGGTACAAACGAG	CAGATGGATCAGCCAAGAAGG	qRT-PCR
SNAI1	NM_005985	TAGCGAGTGGTCTTCTGCG	AGGGCTGCTGGAAGGTAAAC	qRT-PCR
SNAI2	NM_003068	ACAGCGAACTGGACACACAT	GCGGTAGTCCACACAGTGAT	qRT-PCR
IPO5	NM_178310	AGGTCCTCCCACTGGTTG	AATTGCCTCGTGCATTCTC	qRT-PCR

Table 1. Primer sequences used for generation of *in situ* hybridisation probes and for qRT-PCR to detect mouse and human transcripts.

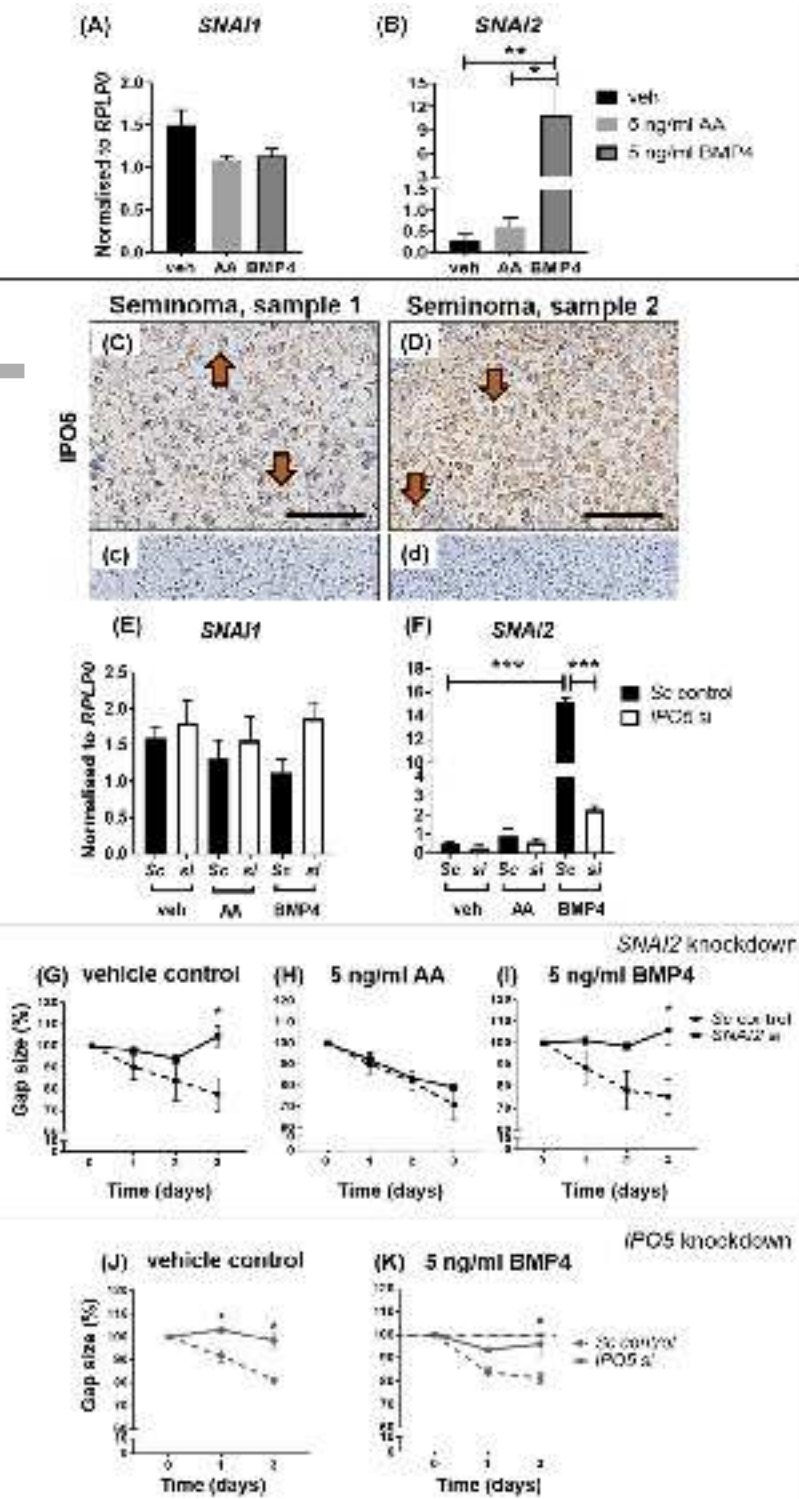




andr_12823_f2.tif



andr_12823_f3.tif



andr_12823_f4.tif



Minerva Access is the Institutional Repository of The University of Melbourne

Author/s:

Micati, DJ; Radhakrishnan, K; Young, JC; Meyts, ER-D; Hime, GR; Abud, HE; Loveland, KL

Title:

'Snail factors in testicular germ cell tumours and their regulation by the BMP4 signalling pathway'

Date:

2020-06-12

Citation:

Micati, D. J., Radhakrishnan, K., Young, J. C., Meyts, E. R. -D., Hime, G. R., Abud, H. E. & Loveland, K. L. (2020). 'Snail factors in testicular germ cell tumours and their regulation by the BMP4 signalling pathway'. ANDROLOGY, 8 (5), pp.1456-1470.

<https://doi.org/10.1111/andr.12823>.

Persistent Link:

<http://hdl.handle.net/11343/275899>

File Description:

Accepted version